A neural network model for determination of the breakdown voltage for separate absorption and multiplication region avalanche photodiode (SAM-APD)

Conference Paper · April 2005

DOI: 10.1109/WOCN.2005.1436013 · Source: IEEE Xplore

CITATIONS
7

READS
153

5 authors, including:

Mohammad Soroosh
Shahid Chamran University of Ahvaz
92 PUBLICATIONS **914** CITATIONS
SEE PROFILE

Farzan Gity
Tyndall National Institute
59 PUBLICATIONS **293** CITATIONS
SEE PROFILE

Mohammad Razaghi
University of Kurdistan
59 PUBLICATIONS **160** CITATIONS
SEE PROFILE

A Neural Network Model for Determination of the Breakdown Voltage for Separate Absorption and Multiplication Region Avalanche Photodiode (SAM-APD)

M. Soroosh[1,2], F. Gity[2], A. R. Sherafat[2], Kh. Farahani[2], M. Razaghi[1,2]

1. Dept. of Optical Systems and Technology, Telecommunication Research Center, Iran, P. O. Box 14155-3961
2. Dept. of Electrical Engineering, School of Engineering, Tarbiat Modares University, Tehran, Iran
Phone: +098-21-8497597, Fax: +98-21-7635588, Email : msoroosh@modares.ac.ir

***Abstract*-In this paper, using the multi layer perceptron (MLP) neural network, we determine the breakdown voltage for separate absorption and multiplication region avalanche photodiode (SAM-APD). Also, we analyze the sensitivity of breakdown voltage with different parameters. As examples, five devices are simulated with the model.**

***Keywords*-neural network (NN), separate absorption and multiplication region avalanche photodiode (SAM-APD).**

I. Introduction

Avalanche photodiodes (APDs) are promising for high-gain, high-speed, and low-noise detector applications provided that they exhibit single-carrier-initiated, single-carrier multiplication [1].

It's shown that absorption region requires a separation of the multiplication region in order to achieve low bias voltage and low noise [1]. These separate absorption and multiplication avalanche photodiodes have been widely deployed in long-wavelength and high-bit-rate optical transmission systems.

Breakdown voltage is a serious limitation. An increase of the bias voltage causes the gain to be increased. However, the breakdown may happen. The prediction of breakdown voltage is very important when increasing the gain. If the bias voltage exceeds the breakdown, the device is destroyed and information is lost. Obviously, that is not desired and must be avoided.

Until recently, only few models have been reported for the separate absorption and multiplication region avalanche photodiode (SAM-APD) [2-4]. These models can not calculate the breakdown voltage.

In this paper, we present a multi layer perceptron (MLP) neural network model for calculation of the breakdown voltage. Absorption and multiplication widths, energy band gap and doping concentration of absorption and multiplication regions are the most important parameters that have a great influence on breakdown voltage. These parameters are the inputs and the breakdown voltage is the output of the network.

We can use this model, before fabrication, in order to determine the breakdown voltage with different parameters of the device. Therefore, we can achieve the optimum case and change the parameters.

II. SAM-APD Structure

The schematic structure of SAM-APD is shown in Fig. 1. Our deductions are based on the illumination through p-side (ITPS). The incident photons are absorbed in p^+, i, and m regions. The current which flows through the interfaces p^+-i and n^+-m, includes two parts: one is diffusion current of the minority carriers in the n^+ and p^+ regions, and the other is the drift current for i and m regions. Because of the high electric field, the impact ionization takes place in the m region.

III. MLP Neural Network

Neural network is one of the most important methods of artificial intelligence that mimics the characteristics of the human brain and during the training process, extracts the inner knowledge of data, saves and generalizes them in other situations.

In the case of nonlinear mapping, the MLP network with back propagation error training algorithm is the most popular neural network. It consists of an input layer, one or more hidden layer(s) and an output layer (Fig. 2).

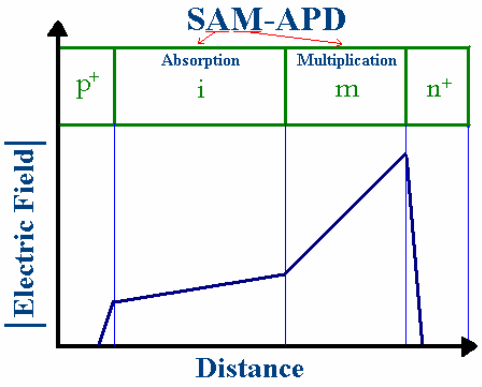

Fig. 1. Schematic drawing of SAM-APD.

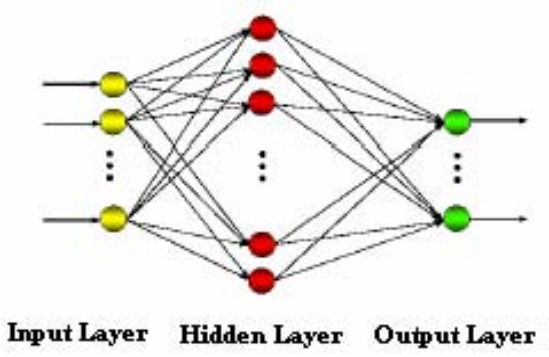

Fig. 2. Multi layer perceptron neural network.

The good behavior is always encouraged and the wrong behavior is punished. The back propagation method utilizes this concept. At first, the input pattern is presented to the network and then the output is computed. The error of the output is computed by the comparison between the computed and desired (target) output. This error is back propagated from each layer to the previous one. The improvement in weights is related to the amount of this error.

In this paper, we set six inputs and one output to the network. Inputs include absorption and multiplication widths, energy band gap and doping concentration of absorption and multiplication regions. The output is the breakdown voltage.

A. Data and Normalization

In our study, 57 experiment patterns have been used: 52 patterns for network training and 5 patterns for network testing [5-26]. Each pattern consists of six input elements and one output element.

In order to normalize the data, all the patterns are transformed into the range of [0.05,0.95]. The following formula is used for normalization of data:

$$X_n = 0.05 + 0.9\frac{X_r - X_{\min}}{X_{\max} - X_{\min}}. \quad (1)$$

where X_n and X_r are normalized and unnormalized input and X_{min} and X_{max} are minimum and maximum of input range, respectively.

B. Network Architecture

A trial and error process is used to achieve the optimum case (meaning the number of neurons in the hidden layer and the type of activation function) [6-10,12,14-21,23-26]. In the hidden layer used in this process the number of neurons tested varied from 2 to 15. In order to evaluate the effect of the activation function on the network performance, four different cases were investigated as follows:

Case1: sigmoid activation function in all layers.
Case2: hyperbolic tangent activation function in all layers.
Case3: linear activation function in all layers.
Case4: sinusoidal activation function in all layers.

Number of epochs is 120000. The RMS error was obtained from the training set. It was observed that the 6-6-1 MLP network (i.e. 6 input neurons, 6 hidden neurons, and 1 output neuron) with sigmoid activation function in all layers is the best choice (Fig. 3).

In order to avoid over training, a sensitivity analysis is used to find the optimal number of epochs. So the 6-6-1 MLP network with sigmoid activation function is evaluated for different numbers of epochs (Fig. 4). This figure shows that when more than 120000 epochs are used, performance of the model is not improved.

IV. Model Validation

In this part, the performance of the developed model is evaluated using the testing data set [1,5,11,13,22]. These data were not used in the training process.

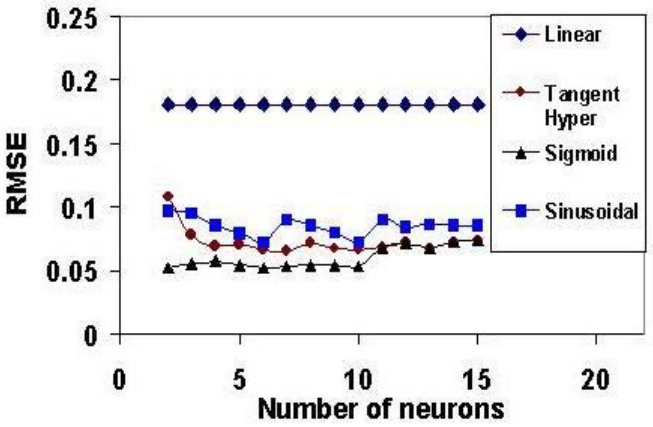

Fig. 3. The RMSE with different numbers of hidden neurons and activation functions.

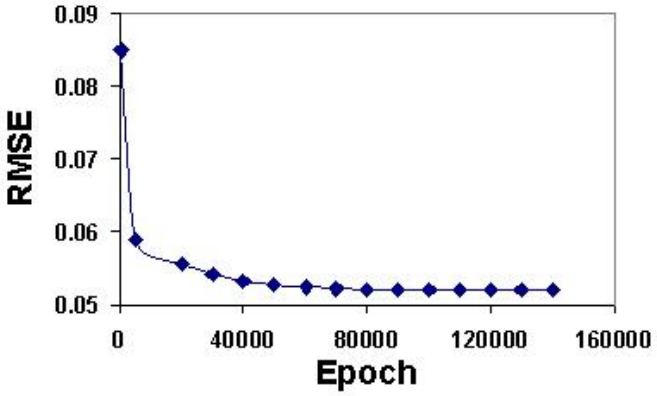

Fig. 4. RMSE with different numbers of epochs.

Fig. 5 shows the results of our model compared to the experiment results for 5 sample devices [1,5,11,13,22]. The neural network (NN) model results are presented versus the experiment results (Fig. 5-a). Also, the difference between the results is demonstrated in Fig. 5-b. It was seen that the NN results are in good agreement with the experiment.

For sensitivity analysis, we changed one of the inputs in the range of [0.05,0.95] while others remained unchanged (Fig. 6) [10]. Evidently, the greater the slope of the curve the greater the sensitivity of the breakdown voltage. Breakdown voltage is more sensitive to multiplication width (W_m), absorption width (W_i), band gap of multiplication region (E_{gm}), doping concentration in multiplication region (N_m), doping concentration in the absorption region (N_i), and band gap of absorption region (E_{gi}).

Clearly, an increase in the multiplication and absorption widths causes the device to become wider. Hence, the breakdown voltage is increased. When the type of the material used in the multiplication region is changed, its characteristics change as well.

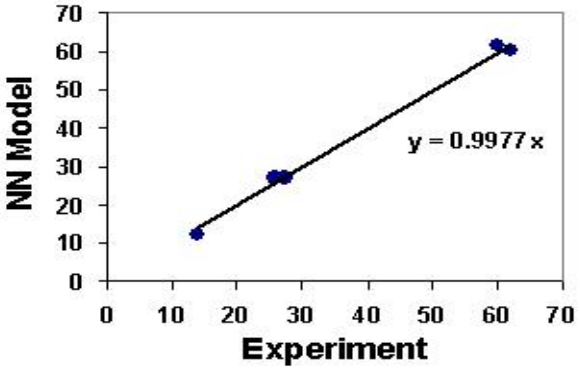

(a)

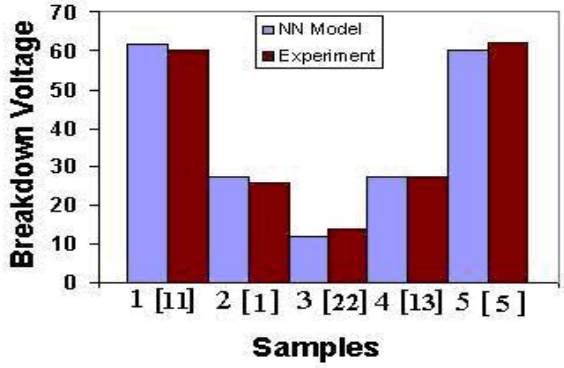

(b)

Fig. 5. A comparison between the NN Model results and experiment results: (a) the NN Model versus experiment. (b) column presentation for the NN Model and experiment.

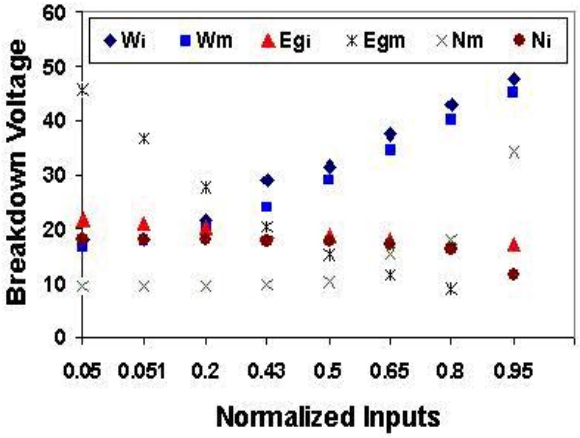

Fig. 6. Breakdown voltage versus normalized inputs.

The conductivity of the multiplication region is proportional to its doping concentration. An increase in the concentration of the multiplication region leads to a bigger electric field in the absorption region. The absorption region, known to be wider than the multiplication region, can accept a higher voltage. However, a greater concentration in the multiplication region will raise the amplitude of the electric field in the interface between the multiplication and n^+ regions. Among the above parameters the first one is the dominant.

An increase in the doping concentration in the absorption region sets the electric field in the multiplication region. Therefore, the breakdown voltage is decreased with increase of N_i. The effect of the type of the absorption material on the breakdown voltage is insignificant.

Our model can predict the breakdown voltage examined against different sizes of the two regions. For illustration, we have presented a number of examination results below. The effects of the absorption region width and the concentration of the multiplication region on the breakdown voltage with different multiplication widths are shown in Figs. 7 and 8 [10].

These results agree with the sensitivity analysis (Fig. 6). The breakdown voltage versus the absorption width is shown in Figs. 9 and 10 [10]. These figures show the effect of multiplication width and doping concentration of absorption region for two different values.

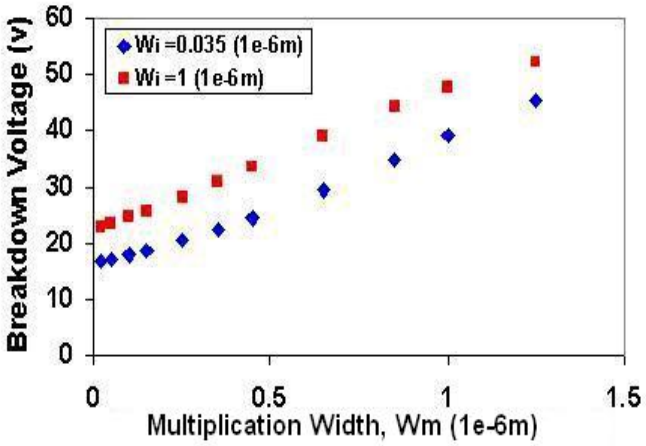

Fig. 7. The breakdown voltage versus the multiplication width and different absorption widths [10].

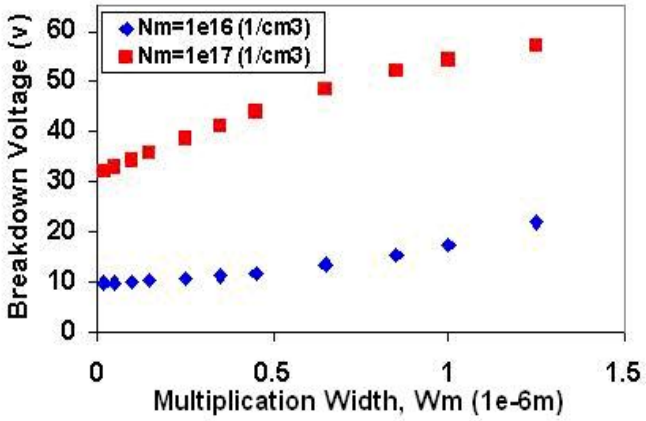

Fig. 8. The breakdown voltage versus the multiplication width and two different concentrations of the multiplication region [10].

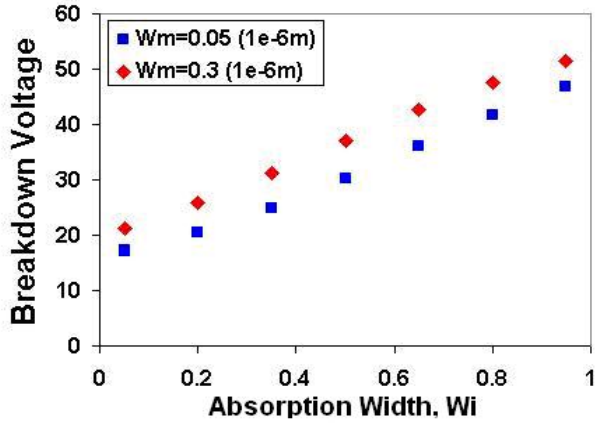

Fig. 9. The breakdown voltage versus the absorption width and two different multiplication widths [10].

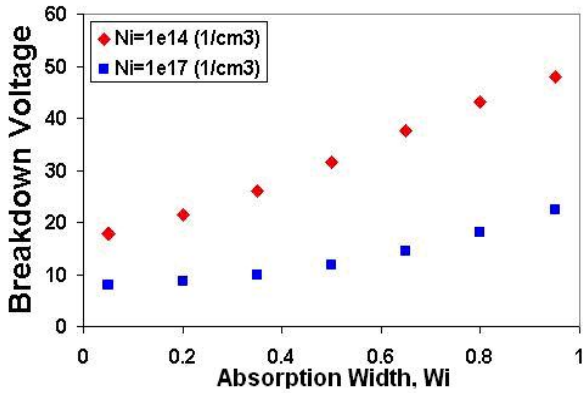

Fig. 10. The breakdown voltage versus the absorption width and two different concentrations of the absorption region [10].

Fig. 11 shows the breakdown voltage versus the concentration of multiplication region for two different concentrations of the absorption region [10].

Figs. 7-11 are compatible with our sensitivity analysis (Fig. 6). A comparison between our model and the experiment results shows that our model is capable of predicting the breakdown voltage against any changes in the value of different parameters, such as the width and the concentration of the multiplication and absorption regions.

V. Conclusion

In our study we have presented a new neural network methodology capable of determining the breakdown voltage. Comparing the results of the experimented data with the results of our model we found that our model has the desired performance. We also concluded that our proposed method has significant advantages in predicting the breakdown voltage of the device before fabrication.

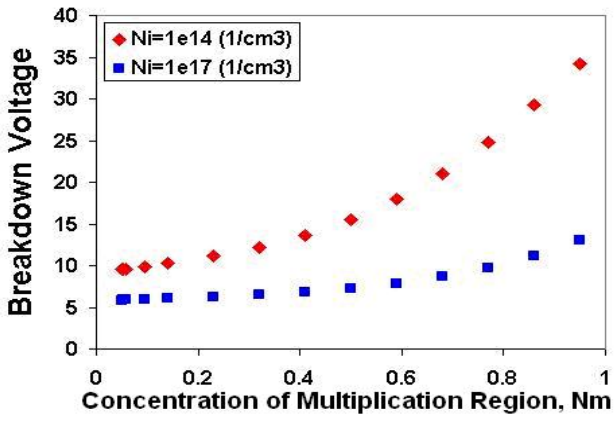

Fig. 11. The breakdown voltage with the concentration of multiplication region and two different concentrations of the absorption region [10].

REFERENCES

[1] Y. Kang, P. Mages, and A. R. Glawson, "Fused InGaAs-Si avalanche photodiodes with low-noise performances," IEEE Photon. Technol. Lett., vol.14, pp. 1593-1595, 2002.

[2] M. Soroosh, A. Zarifkar, M. Razaghi, and M. K. Moravvej-Farshi, "Separate absorption and multiplication avalanche photodiode (SAM-APD) model for circuit simulation", IEEE Gulf International Conference (GCC), pp. 606-611, Bahrain, 2004.

[3] A. Zarifkar and M. Soroosh, "Circuit modeling of separate absorption, charge and multiplication avalanche photodiode (SACM-APD)," 6th International Conference on Laser and Fiber-Optical Network Modeling (LFNM), pp. 213-219, Ukrain, 2004.

[4] M. Soroosh, A. Zarifkar, M. Razaghi, and M. K. Moravvej-Farshi, "A neural network model for determination of excess noise factor for separate absorption and multiplication region avalanche photodiode," International Conference on Optics and Photonics(ICO), pp. 403-404, Japan, 2004.

[5] G. Hasnain, Wayne G. Bi, S. Song, John T. Anderson, N. Moll, C. Su, James N. Hollenhorst, Nicholas D. Baynes, I. Athroll, Sean Amos, and R. M. Ash, "Buried-mesa avalanche photodiodes," IEEE J. Quantum Electron., vol. 34, No. 12, pp. 2321-2326, Dec. 1998.

[6] H. Nie, K. A. Anselm, C. Lenox, P. Yuan, C. Hu, G. Kinsey, B. G. Streetman, and J. C. Campbel, "Resonant-cavity separate absorption, charge and multiplication avalanche photodiodes with high-speed and high gain-bandwidth product," IEEE Photon. Tech. Lett., vol. 10, No. 3, pp. 409-411, March 1998.

[7] K. A. Anselm, S. S. Murtaza, C. Hu, H. Nie, B. G. Streetman, and J. C. Campbell, "A resonant-cavity, separate-absorption-and-multiplication, avalanche photodiode with low excess noise factor," IEEE Electron Device Lett., vol. 17, No. 3, pp. 91-93, March 1996.

[8] Yegao G. Xiao, and M. Jamal Deen, "Modeling of two-dimensional gain profiles for InP–InGaAs avalanche photodiodes with a stochastic approach," IEEE J. Quantum Electron., vol. 35, No. 12, pp. 1853-1862, Dec. 1999.

[9] Joe N. Haralson, and Kevin F. Brennan, "Novel edge suppression technique for planar avalanche photodiodes," IEEE J. Quantum Electron., vol. 35, No. 12, pp. 1863-1869, Dec. 1999.

[10] H. Nie, K.A. Anselm, C. Hu, C. Lenox, B.G. Streetman, J. C. Campbell, "High-speed resonant-cavity SAM avalanche photodiodes," Research in University of Texas, 1998.

[11] J. Wei, J. C. Dries, H. Wang, G. H. Olsen, and S. R. Forrest, "Optimization of double diffused floating guarding ring InGaAs/InP avalanche photodiodes," Research in Princeton University, 2001.

[12] J. Yao, K. K. Loi, P. Baret, S. Kwan, and M. A. Itzler, "Bandwidth simulation of 10 Gb/s avalanche photodiodes," Research in New Jersey University, 2001.

[13] C. Hu, K. A. Anselm, B. G. Streetman, and J. C. Campbell, "Excess noise in GaAs avalanche photodiodes with thin multiplication regions," IEEE J. Quantum Electron., vol. 33, No. 7, pp. 1089-1093, July. 1997.

[14] J. C. Dries, T. Martin, W. Huang, M. J. Lange, and M. J. Cohen, "Two-dimensional InGaAs avalanche photodiode arrays for high sensitivity, high speed imaging," Research in Princeton University, 2002.

[15] D. Hasko, F. Uherek, and F. Mika, "InGaAs/InP avalanche photodiodes with a thin multiplication layer," Research in the Slovak University of Technology, 2002.

[16] M. D. A. Mac Bean, N. P. Hewett, M. D. Learmouth, and I. Reid, "Planar InP/InGaAs avalanche photodetector with integrated dielectric wavelength filter," Electronics Lett., vol. 26, No. 12, pp. 804-806, June 1990.

[17] Y. Liu, S. R. Forrest, J. Hladky, M. J. Lange, G. H. Osen, and D. E. Ackley, "A planar InP/InGaAs avalanche photodiode with floating guard ring and double diffused junction," IEEE J. Lightwave Tech., vol. 10, No. 2, pp. 182-193, Feb. 1992.

[18] J. Harari, D. Decoster, J. P. Vilcot, B. Kramer, C. Oguey, P. Salsac, and G. Ripoche, "Numerical simulation of avalanche photodiodes with guard ring," IEE Proceeding-J, vol. 138, No. 3, pp. 211-217, June 1991.

[19] M. D. A. Mac Bean, P. M. Rodgers, T. G. Lynch, M. Learmouth, R. H. Walling, and M. J. Robertson, "Planar InP/InGaAs avalanche photodiodes fabricated using Si implantation and two stage atmospheric pressure MOVPE," Research in British Telecom Research Laboratories, 1994.

[20] C. L. F. Ma, M. J. Deen, and L. E. Tarof, "Multiplication in separate absorption, grading, charge, and multiplication InP-InGaAs avalanche photodiodes," IEEE J. Quantum Electron., vol. 31, No. 11, pp. 2078-2089, Nov. 1995.

[21] C. L. F. Ma, M. J. Deen, L. E. Tarof, and J. C. H. Yu, "Temperature dependence of breakdown voltage in separate absorption, grading, charge, and multiplication InP/InGaAs avalanche photodiodes," IEEE Trans. Electron Devices, vol. 42, No. 5, pp. 810-818, May 1995.

[22] S. S. Murtaza, K. A. Anselm, C. Hu, H. Nie, B. G. Streetman, and C. Campbell, "Resonant-cavity enhanced (RCE) separate absorption and multiplication (SAM) avalanche photodetector (APD)," IEEE Photon. Tech. Lett., vol. 7, No. 12, pp. 1486-1488, Dec. 1995.

[23] C. L. F. Ma, M. J. Deen, and L. E. Tarof, "D.C. and noise characteristics of InP-based avalanche photodiodes for optical communication applications," Research in Simon Fraser University and Bell-Northern Research Ltd., 1993.

[24] A. Bandyopadhyay, M. J. Deen, L. E. Tarof, and W. Clark, "A simplified approach to time-domain modeling of avalanche photodiodes," IEEE J. Quantum Electron., vol. 34, No. 4, pp. 691-699, Apr. 1998.

[25] Y. Kang, P. Mages, A. Pauchard, A. R. Clawson, S. S. Lau, Y. H. Lo, and P. K. L. Yu, "Dark current reduction in fused InGaAs/Si avalanche photodiode," Research in University of California, San Diego and Nova Crystals Inc., 2001.

[26] J. Yu, L. E. Tarof, R. Bruce, D. G. Knight, K. Visvanatha, and T. Baird, "Noise performance of separate absorption, grading, charge and multiplication InP/InGaAs avalanche photodiodes," IEEE Photon. Tech. Lett., vol. 6, No. 5, pp. 632-634, May 1994.